Regular Article - Theoretical Physics

Form factors of decuplet baryons in a covariant quark–diquark approach

JiaQi Wang[1,2,a], **Dongyan Fu**[1,2,b], **Yubing Dong**[1,2,c]

[1] Institute of High Energy Physics, Chinese Academy of Sciences, Beijing 100049, China
[2] School of Physical Sciences, University of Chinese Academy of Sciences, Beijing 101408, China

Abstract The electromagnetic and gravitational form factors of decuplet baryons are systematically studied with a covariant quark–diquark approach. The model parameters are firstly discussed and determined through comparison with the lattice calculation results integrally. Then, the electromagnetic properties of the systems including electromagnetic radii, magnetic moments, and electric-quadrupole moments are calculated. The obtained results are in agreement with experimental measurements and the results of other models. Finally, the gravitational form factors and the mechanical properties of the decuplet baryons, such as mass radii, energy densities, and spin distributions, are also calculated and discussed.

1 Introduction

Form factors (FFs) provide a wealth of information for understanding the inner structures of particles. Electromagnetic form factors (EMFFs) can provide the electromagnetic properties of a system, such as its charge radius, magnetic moment, and even higher-order moments. Meanwhile, gravitational form factors (GFFs), which are derived from the matrix element of the symmetric energy–momentum tensor [1], can give the mechanical properties, such as the mass and angular momentum distributions.

The spin-3/2 particle is the main research object of this work. The most fundamental spin-3/2 particles, including $\Delta(1232)$, $\Sigma(1385)$, $\Xi(1530)$, and Ω^-, are known as the decuplet baryons with SU(3) symmetry, and it is important to investigate them systematically. The composition of the decuplets is illustrated in Fig. 1. The Δ resonance, as the

lowest excited state of the nucleon, has been considered as a typical target in the research of spin-3/2 particles. Unfortunately, due to the short lifetime [2] of the Δ isobar, directly measuring its EMFFs experimentally remains a challenge. In the decuplets, Σ^* and Ξ^* have a similar short lifetime, while Ω^- has a longer lifetime, with $c\tau = 2.461$ cm [2]. Fortunately, the transition processes can be expected to yield information on accessing the electromagnetic properties of Δ and other decuplet baryons [3–5]. Additionally, the magnetic moments of Δ^{++} and Δ^+ have been measured through $\pi^+ p \to \pi^+ p\gamma$ [6] and $\gamma p \to \pi^0 p\gamma'$ [7] processes. Since Ω^- has a longer lifetime, there are more opportunities to directly probe its structure, and its time-like form factors and effective form factors have been measured by CLEO [8] and BESIII [9] through the process of $e^+e^- \to \Omega^-\overline{\Omega}^+$. Furthermore, we expect that new experimental facilities may provide us more useful data to understand the electromagnetic structures of the decuplets. For example, BESIII and possible future super J/ψ factory SCTF are expected to implement the secondary beam of Ω^- through a $\psi(2S) \to \Omega^-\overline{\Omega}^+$ process [10], and JLab (Jefferson Lab) is planning to measure the electromagnetic properties of Σ^* and Ξ^* in future experiments [11,12].

Although some experimental facilities are working on the EMFFs of the decuplet baryons, it is still hard to measure their GFFs directly due to their negligible gravitational interaction. However, GFFs can be extracted from generalized parton distributions [13–16] and generalized distribution amplitudes [17]. With respect to the nucleon, generalized parton distributions are expected to be measured from deeply virtual Compton scattering [18] at some facilities including JLab [19], the future EIC (Electron Ion Collider) [20], and the EicC (Electron-Ion Collider in China) [21].

There have been numerous theoretical works about the FFs of hadrons over the past decades, including those with targets
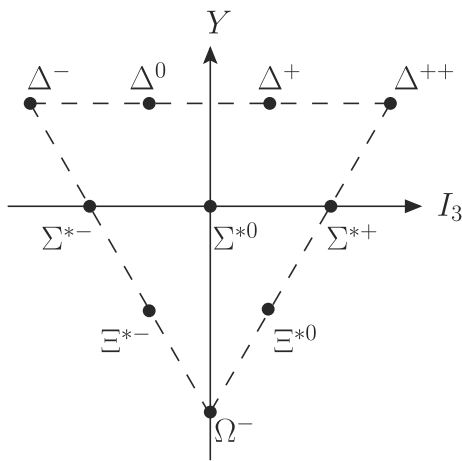
Fig. 1 Members of the decuplet baryons

of spin-0 [17,22–24], spin-1/2 [25–31], and spin-1 [15,32–35]. The electromagnetic properties of decuplets with spin-3/2 have also been studied with various approaches, such as lattice QCD (LQCD) [36–41], the Skyrme model [42], chiral perturbation theories (χPT) [43,44], quark models [45–47], QCD sum rules [48–50], the chiral constituent quark model (χCQM) [51], $1/N_c$ expansion [52,53], the general QCD parameterization method (GPM) [54,55], and the chiral quark soliton model (χQSM) [56]. In terms of the GFFs of spin-3/2 particles, studies on Δ [57–60] and Ω^- [61] have been carried out. However, systematic studies on the GFFs of the whole decuplets are still lacking.

To study the EMFFs and GFFs of the decuplet baryons simultaneously, we adopt a relativistic and covariant quark–diquark approach. In this model, we treat the three-body system of a decuplet as a two-body system composed of a quark and a spin-1 (axial-vector) diquark. Therefore, this approach significantly simplifies the numerical calculations. Moreover, we explicitly take account of the diquark internal structure to obtain more accurate results. In our previous works, this model has been employed for two typical baryons, Δ resonance [59] and Ω^- [61], and we believe that it will be more efficient and simpler when studying the $N - \Delta$ transition process in our future work. Recall that the determination of model parameters employed in Refs. [59,61] is based on fitting to the LQCD results of Δ (the u and d quark system) and Ω^- (the s quark system), respectively. In order to provide a systematic description of all the decuplet baryons built from u, d, and s quarks, a new set of model parameters is determined. Then, the EMFFs and GFFs of the systems are calculated.

The remainder of this paper is organized as follows. Section 2 briefly presents the definitions of the EMFFs and GFFs of a spin-3/2 particle and introduces our covariant quark–diquark approach. In Sect. 3, the model parameters used in this calculation for the decuplet baryons are discussed

and determined. With these parameters, the electromagnetic properties obtained for the systems, including electromagnetic multipole moments and radii, are explicitly listed, and our results are compared with other model calculations. Similarly, the GFFs are calculated and the mechanical properties including the mass radii, energy distributions, and angular momentum distributions in the coordinate space are discussed. Finally, Sect. 4 is devoted to a brief summary and some discussion.

2 Form factors and quark–diquark approach

2.1 Electromagnetic form factors

For a spin-3/2 particle, the matrix element of the electromagnetic current can be parameterized as [62]

$$
\begin{aligned}
&\left\langle p', \lambda' \left| \hat{J}_a^\mu (0) \right| p, \lambda \right\rangle \\
&= -\bar{u}_{\alpha'} \left(p', \lambda'\right) \left[\frac{P^\mu}{M} \left(g^{\alpha'\alpha} F_{1,0}^{V,a}(t) - \frac{q^{\alpha'} q^\alpha}{2M^2} F_{1,1}^{V,a}(t) \right) \right. \\
&\quad \left. + \frac{i\sigma^{\mu q}}{2M} \left(g^{\alpha'\alpha} F_{2,0}^{V,a}(t) - \frac{q^{\alpha'} q^\alpha}{2M^2} F_{2,1}^{V,a}(t) \right) \right] u_\alpha (p, \lambda),
\end{aligned}
\tag{1}
$$

where $i\sigma^{\mu q} = i\sigma^{\mu\rho} q_\rho$, M stands for the baryon mass and $u_\alpha (p, \lambda)$ is the Rarita–Schwinger spinor with normalization as $\bar{u}_{\sigma'}(p) u_\sigma(p) = -2M\delta_{\sigma'\sigma}$. The kinematic variables introduced in Eq. (1) are defined as $P^\mu = \left(p^\mu + p'^\mu\right)/2$, $q^\mu = p'^\mu - p^\mu$, and $t = -q^2$, where p (p') is the initial (final) momentum. The index a in $F_{i,j}^{V,a}$ runs from the quark to the gluon, and the total form factor is their sum. In this work, we consider only the constituent quark contribution.

In the Breit frame, the average of the baryon momenta and the momentum transfer are defined as $P = (E, 0)$ and $q = (0, \boldsymbol{q})$, where E is the energy carried by the baryon. Then, the EMFFs of a spin-3/2 particle can be expressed in terms of $F_{i,j}^V$ [63]

$$
\begin{aligned}
G_{E0}(t) = \left(1 + \frac{2}{3}\tau\right) &[F_{2,0}^V(t) + (1+\tau)(F_{1,0}^V(t) - F_{2,0}^V(t))] \\
&+ \frac{2}{3}\tau(1+\tau)[F_{2,1}^V(t) + (1+\tau)(F_{1,1}^V(t) - F_{2,1}^V(t))],
\end{aligned}
\tag{2a}
$$

$$
\begin{aligned}
G_{E2}(t) = &[F_{2,0}^V(t) + (1+\tau)(F_{1,0}^V(t) - F_{2,0}^V(t))] \\
&+ (1+\tau)[F_{2,1}^V(t) + (1+\tau)(F_{1,1}^V(t) - F_{2,1}^V(t))],
\end{aligned}
\tag{2b}
$$

$$
G_{M1}(t) = \left(1 + \frac{4}{5}\tau\right) F_{2,0}^V(t) + \frac{4}{5}\tau(\tau + 1) F_{2,1}^V(t),
\tag{2c}
$$

$$
G_{M3}(t) = F_{2,0}^V(t) + (\tau + 1) F_{2,1}^V(t),
\tag{2d}
$$

where $\tau = -t/(4M^2)$, with $t < 0$. In Eq. (2), G_{E0}, G_{E2}, G_{M1}, and G_{M3} respectively represent the electric-monopole, electric-quadrupole, magnetic-dipole, and magnetic-octupole form factors. When the squared momentum transfer t goes to 0, the electric charge Q_e, magnetic moment μ, electric-quadrupole moment $\mathcal{Q}$, and magnetic-octupole moment $\mathcal{O}$ can be obtained through [64]

$$Q_e = G_{E0}(0), \quad \mu = \frac{e}{2M}G_{M1}(0),$$
$$\mathcal{Q} = \frac{e}{M^2}G_{E2}(0), \quad \mathcal{O} = \frac{e}{2M^3}G_{M3}(0). \tag{3}$$

The electric charge and magnetic radii are defined from their corresponding form factors as [40][1]

$$\langle r^2\rangle_{E0} = \frac{6}{G_{E0}(0)}\frac{\mathrm{d}}{\mathrm{d}t}G_{E0}(t)\bigg|_{t=0},$$
$$\langle r^2\rangle_{M1} = \frac{6}{G_{M1}(0)}\frac{\mathrm{d}}{\mathrm{d}t}G_{M1}(t)\bigg|_{t=0}. \tag{4}$$

2.2 Gravitational form factors

The GFFs can be calculated from the matrix element of the energy–momentum tensor $\hat{T}^{\mu\nu}$ as [62]

$$
\begin{aligned}
&\left\langle p', \lambda' \left| \hat{T}_a^{\mu\nu}(0) \right| p, \lambda \right\rangle \\
&= -\bar{u}_{\alpha'}\left(p', \lambda'\right)\Bigg[\frac{P^\mu P^\nu}{M}\left(g^{\alpha'\alpha}F_{1,0}^{T,a}(t) - \frac{q^{\alpha'}q^\alpha}{2M^2}F_{1,1}^{T,a}(t)\right) \\
&\quad + \frac{(q^\mu q^\nu - g^{\mu\nu}q^2)}{4M}\left(g^{\alpha'\alpha}F_{2,0}^{T,a}(t) - \frac{q^{\alpha'}q^\alpha}{2M^2}F_{2,1}^{T,a}(t)\right) \\
&\quad + Mg^{\mu\nu}\left(g^{\alpha'\alpha}F_{3,0}^{T,a}(t) - \frac{q^{\alpha'}q^\alpha}{2M^2}F_{3,1}^{T,a}(t)\right) \\
&\quad + \frac{iP^{\{\mu}\sigma^{\nu\}\rho}q_\rho}{2M}\left(g^{\alpha'\alpha}F_{4,0}^{T,a}(t) - \frac{q^{\alpha'}q^\alpha}{2M^2}F_{4,1}^{T,a}(t)\right) \\
&\quad - \frac{1}{M}\left(q^{\{\mu}g^{\nu\}\{\alpha'}q^{\alpha\}} - 2q^{\alpha'}q^\alpha g^{\mu\nu} \right. \\
&\quad \left. - g^{\alpha'\{\mu}g^{\nu\}\alpha}q^2 \right)F_{5,0}^{T,a}(t) \\
&\quad + Mg^{\alpha'\{\mu}g^{\nu\}\alpha}F_{6,0}^{T,a}(t)\Bigg]u_\alpha(p, \lambda), \tag{5}
\end{aligned}
$$

where the convention $a^{\{\mu}b^{\nu\}} = a^\mu b^\nu + a^\nu b^\mu$ is used. Note that $F_{3,0}^T$, $F_{3,1}^T$ and $F_{6,0}^T$ are the non-conserving terms which will vanish when considering the contribution from the gluon, so we simply ignore them here.

Analogously to the EMFFs, the gravitational multipole form factors (GMFFs), including the energy-monopole

(-quadrupole) form factors $\varepsilon_{0(2)}(t)$, the angular momentum-dipole (-octupole) form factors $\mathcal{J}_{1(3)}(t)$, and the form factors $D_{0,2,3}(t)$, can be expressed as the linear combination of the GFFs, $F_{i,j}^T(t)$. The detailed definitions of the GMFFs have been explicitly given in Ref. [57], and thus we do not repeat them to avoid verbosity. Moreover, the mass radius of a baryon is obtained through the energy-monopole form factor as

$$\langle r^2\rangle_M = \frac{6}{\varepsilon_0(0)}\frac{\mathrm{d}}{\mathrm{d}t}\varepsilon_0(t)\bigg|_{t=0}. \tag{6}$$

The energy, angular momentum, and mechanical force densities of the baryons in the coordinate space (r-space) can be derived through Fourier transformation into the corresponding form factors. The energy-monopole and energy-quadrupole densities are defined as [57]

$$\mathcal{E}_0(r) = M\widetilde{\varepsilon}_0(r), \quad \mathcal{E}_2(r) = -\frac{1}{M}r\frac{\mathrm{d}}{\mathrm{d}r}\frac{1}{r}\frac{\mathrm{d}}{\mathrm{d}r}\widetilde{\varepsilon}_2(r), \tag{7}$$

with

$$\widetilde{\varepsilon}_{0,2}(r) = \int\frac{d^3q}{(2\pi)^3}e^{-i\boldsymbol{q}\cdot\boldsymbol{r}}\varepsilon_{0,2}(t), \tag{8}$$

being the densities in r-space. The angular momentum density can be expressed as

$$\rho_J(r) = -\frac{1}{3}r\frac{\mathrm{d}}{\mathrm{d}r}\int\frac{d^3q}{(2\pi)^3}e^{-i\boldsymbol{q}\cdot\boldsymbol{r}}\mathcal{J}_1(t). \tag{9}$$

According to Ref. [1], it is argued that the densities of the corresponding pressure and shear force in classical medium physics are derived from the form factors correlated with the "D-term" as

$$p_0(r) = \frac{1}{6M}\frac{1}{r^2}\frac{\mathrm{d}}{\mathrm{d}r}r^2\frac{\mathrm{d}}{\mathrm{d}r}\tilde{D}_0(r),$$
$$s_0(r) = -\frac{1}{4M}r\frac{\mathrm{d}}{\mathrm{d}r}\frac{1}{r}\frac{\mathrm{d}}{\mathrm{d}r}\tilde{D}_0(r), \tag{10}$$

where

$$\tilde{D}_0(r) = \int\frac{\mathrm{d}^3q}{(2\pi)^3}e^{-i\boldsymbol{q}\cdot\boldsymbol{r}}D_0(t). \tag{11}$$

The higher-order pressures and shear forces are omitted here and explicitly listed in Ref. [57].

2.3 Quark–diquark approach

We know that the decuplet baryons are composed of three quarks and have a spin of 3/2. In our quark–diquark approach, we treat the baryon as a bound state of a spin-1/2 quark and a spin-1 (axial-vector) diquark. The SU(6) spin-flavor wave functions of the decuplets are listed in Appendix A [65]. According to the wave functions, the total matrix element can be expressed as the sum of the quark and

---

[1] For the neutral baryon, the radii are defined as [44]

$$\langle r^2\rangle_{E0} = 6\frac{\mathrm{d}}{\mathrm{d}t}G_{E0}(t)\bigg|_{t=0}, \quad \langle r^2\rangle_{M1} = 6\frac{\mathrm{d}}{\mathrm{d}t}G_{M1}(t)\bigg|_{t=0}.$$

diquark contributions,

$$
\begin{aligned}
\left\langle p', \lambda' \left| \hat{J}^{\mu}(0) \right| p, \lambda \right\rangle &= \left\langle p', \lambda' \left| \hat{J}_q^{\mu}(0) \right| p, \lambda \right\rangle \\
&+ \left\langle p', \lambda' \left| \hat{J}_D^{\mu}(0) \right| p, \lambda \right\rangle.
\end{aligned}
\tag{12}
$$

Figure 2 gives the Feynman diagrams for the electromagnetic interaction. One can write the contribution of the quark according to Fig. 2a as

$$
\begin{aligned}
\left\langle p', \lambda' \left| \hat{J}_q^{\mu}(0) \right| p, \lambda \right\rangle &= -Q_e^q e \bar{u}_{\alpha'}(p', \lambda') \left(-i \mathcal{C}^2 \right) \\
&\times \int \frac{d^4 l}{(2\pi)^4} \frac{1}{\mathfrak{D}} \Gamma^{\alpha'\beta'} \left(\slashed{l} + \frac{\slashed{q}}{2} + m_q \right) g_{\beta'\beta} \gamma^{\mu} \\
&\times \left(\slashed{l} - \frac{\slashed{q}}{2} + m_q \right) \Gamma^{\alpha\beta} u_{\alpha}(p, \lambda),
\end{aligned}
\tag{13}
$$

where Q_e^q is the electric charge carried by the quark, $\mathcal{C}$ is a normalization constant to ensure the calculated result $G_{E0}^q(0) = Q_e^q$, and $\Gamma^{\alpha\beta}$ is the vertex of the baryon with its quark and diquark constituents. Note in particular that we neglect the $k^{\mu} k^{\nu}/m_D^2$ term in the propagator of the diquark (1^+) to avoid divergence of the integral [66]. According to Ref. [67], the Lorentz structure of the vertex is

$$
\Gamma^{\alpha\beta} = g^{\alpha\beta} + c_2 \gamma^{\beta} \Lambda^{\alpha} + c_3 \Lambda^{\beta} \Lambda^{\alpha},
\tag{14}
$$

where Λ is the relative momentum between the quark and the diquark. The parameters of couplings c_2, c_3 in Eq. (14) can be determined by fitting to the lattice data [36,37], and we assume that they are independent of the baryon mass. $\mathfrak{D}$ in Eq. (13) contains the denominators of the propagators and a special scalar function ζ attached to the vertex to ensure that the quark and the diquark can form a bound state. Here we simply choose the function [68]

$$
\zeta(p_1, p_2) = \frac{\mathcal{C}}{\left[p_1^2 - m_R^2 + i\epsilon \right] \left[p_2^2 - m_R^2 + i\epsilon \right]},
\tag{15}
$$

with m_R as a cutoff parameter which is positively correlated with the baryon mass. The total $\mathfrak{D}$ is thus written as

$$
\begin{aligned}
\mathfrak{D} &= \left[(l - P)^2 - m_R^2 + i\epsilon \right]^2 \left[\left(l - \frac{q}{2} \right)^2 - m_R^2 + i\epsilon \right] \\
&\times \left[\left(l + \frac{q}{2} \right)^2 - m_R^2 + i\epsilon \right] \\
&\times \left[\left(l + \frac{q}{2} \right)^2 - m_q^2 + i\epsilon \right] \left[\left(l - \frac{q}{2} \right)^2 - m_q^2 + i\epsilon \right] \\
&\times \left[(l - P)^2 - m_D^2 + i\epsilon \right].
\end{aligned}
\tag{16}
$$

Similarly, the diquark contribution Fig. 2b can be expressed as

$$
\begin{aligned}
\left\langle p', \lambda' \left| \hat{J}_D^{\mu}(0) \right| p, \lambda \right\rangle &= -Q_e^D e \bar{u}_{\alpha'}(p', \lambda') i \mathcal{C}^2 \\
&\times \int \frac{d^4 l}{(2\pi)^4} \frac{1}{\mathfrak{D}'} \Gamma^{\alpha'}_{\beta'} \left(\slashed{P} - \slashed{l} + m_q \right) j_D^{\mu, \beta'\beta} \Gamma^{\alpha}_{\beta} u_{\alpha}(p, \lambda),
\end{aligned}
\tag{17}
$$

where

$$
\begin{aligned}
\mathfrak{D}' &= \left[(l - P)^2 - m_R^2 + i\epsilon \right]^2 \left[\left(l - \frac{q}{2} \right)^2 - m_R^2 + i\epsilon \right] \\
&\times \left[\left(l + \frac{q}{2} \right)^2 - m_R^2 + i\epsilon \right] \\
&\times \left[\left(l + \frac{q}{2} \right)^2 - m_D^2 + i\epsilon \right] \left[\left(l - \frac{q}{2} \right)^2 - m_D^2 + i\epsilon \right] \\
&\times \left[(l - P)^2 - m_q^2 + i\epsilon \right].
\end{aligned}
\tag{18}
$$

$j_D^{\mu,\beta'\beta}$ in the above equation stands for the effective electromagnetic current of the diquark. Considering a diquark composed of quarks q_a and q_b, the electromagnetic current can be derived from

$$
\begin{aligned}
\sum_{i=a,b} \left\langle p'_D, \lambda'_D \left| \hat{J}_{q_i}^{\mu}(0) \right| p_D, \lambda_D \right\rangle \\
= -\epsilon_{\beta'}^* \left(p'_D, \lambda'_D \right) j_D^{\mu, \beta'\beta} \epsilon_{\beta} \left(p_D, \lambda_D \right),
\end{aligned}
\tag{19}
$$

where $\epsilon_{\beta}(p_D, \lambda_D)$ represents the spin-1 diquark field, and the kinematic variables are defined as $P_D^{\mu} = \left(p_D^{\mu} + p_D'^{\mu} \right)/2$, $q_D^{\mu} = p_D'^{\mu} - p_D^{\mu} = q^{\mu}$, and $q_D^2 = -t_D = -t$.

Assuming that the diquark is almost on shell, we can write the matrix element

$$
\begin{aligned}
\left\langle p', \lambda' \left| \hat{J}_{q_i}^{\mu}(0) \right| p, \lambda \right\rangle &= -Q_e^{q_i} e \epsilon_{\beta'}^* (p'_D, \lambda'_D) \left(-i \mathcal{C}_D^2 \right) \\
&\times \int \frac{d^4 l_D}{(2\pi)^4} \frac{1}{\mathfrak{D}_D} \gamma^{\beta'} \left(\slashed{l}_D + \frac{\slashed{q}_D}{2} + m_q \right) \gamma^{\mu} \gamma^{\beta} \\
&\times \left(\slashed{l}_D - \frac{\slashed{q}_D}{2} + m_q \right) \epsilon_{\beta}(p_D, \lambda_D),
\end{aligned}
\tag{20}
$$

where the quark–diquark vertex γ^{β} is borrowed from Ref. [69], $\mathcal{C}_D$ is the normalization constant similar to $\mathcal{C}$, and $\mathfrak{D}_D$ is defined as

$$
\begin{aligned}
\mathfrak{D}_D &= \left[(l_D - P_D)^2 - m_R^2 + i\epsilon \right]^2 \left[\left(l_D - \frac{q_D}{2} \right)^2 - m_R^2 + i\epsilon \right] \\
&\times \left[\left(l_D + \frac{q_D}{2} \right)^2 - m_R^2 + i\epsilon \right] \\
&\times \left[\left(l_D + \frac{q_D}{2} \right)^2 - m_q^2 + i\epsilon \right] \left[\left(l_D - \frac{q_D}{2} \right)^2 - m_q^2 + i\epsilon \right] \\
&\times \left[(l_D - P_D)^2 - m_q^2 + i\epsilon \right].
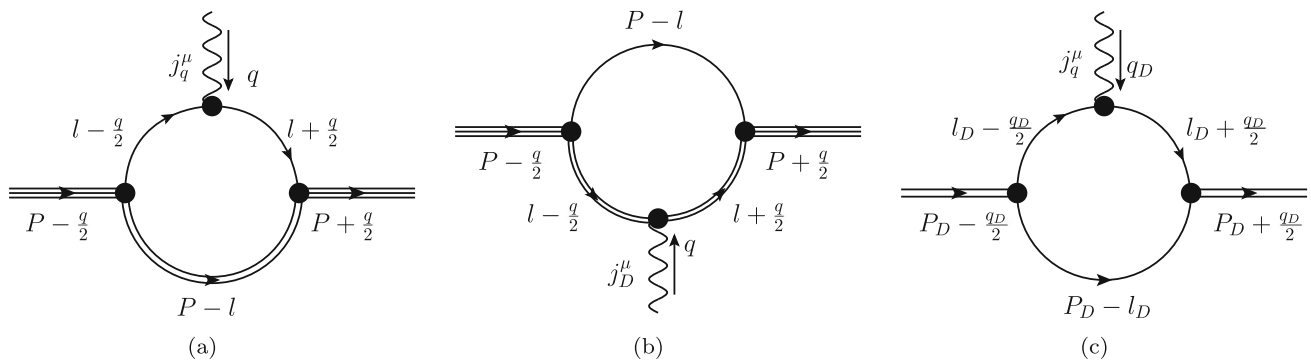\end{aligned}
\tag{21}
$$

Fig. 2 Feynman diagrams for the electromagnetic matrix elements contributed by the quark (**a**) and the diquark (**b**). Diagram **c** gives the internal structure of the diquark in this process

Finally, the effective electromagnetic current $j_D^{\mu,\beta'\beta}$ can be written as

$$j_D^{\mu,\beta'\beta} = \left[g^{\beta'\beta} F_{D,1}^V(t) - \frac{q^{\beta'}q^\beta}{2m_D^2} F_{D,2}^V(t) \right] (p_D' + p_D)^\mu$$
$$- (q^{\beta'} g^{\mu\beta} - q^\beta g^{\mu\beta'}) F_{D,3}^V(t), \qquad (22)$$

where $F_{D,1\,(2,3)}^V(t)$ are the three form factors of the spin-1 diquark.

In terms of the GFFs and according to the quark Lagrangian

$$\mathcal{L} = \frac{i}{2} \overline{\psi}_q \gamma^\mu \overleftrightarrow{\partial}_\mu \psi_q + m_q \overline{\psi}_q \psi_q, \qquad (23)$$

with $\overleftrightarrow{\partial}_\mu = \overrightarrow{\partial}_\mu - \overleftarrow{\partial}_\mu$, we have the symmetric energy–momentum tensor of the quark as

$$T^{\mu\nu} = \frac{i}{4} \overline{\psi}_q \gamma^\mu \overleftrightarrow{\partial}^\nu \psi_q + \frac{i}{4} \overline{\psi}_q \gamma^\nu \overleftrightarrow{\partial}^\mu \psi_q. \qquad (24)$$

Therefore, the GFFs contributed by the quark and the diquark can be calculated by replacing γ^μ with $\gamma^\mu l^\nu + \gamma^\nu l^\mu$ in Eqs. (13) and (20). Our work on $\Delta(1232)$ [59] describes the calculation process in detail.

3 Numerical results

3.1 Parameter determination

Using the on-shell identities in Ref. [62], we can extract the form factors from Eqs. (1) and (5). Before doing the calculation of the loop integrals numerically, it is necessary to input the model parameters including the baryon mass M, quark mass m_q, diquark mass m_D, and the cutoff parameter m_R introduced in Eq. (15). Moreover, the couplings c_2, c_3 in the quark–diquark vertex (14) must also be determined. It should be mentioned that in our previous studies on Δ isobar (the u and d quark system) [59] and Ω^- [61] (the s quark system), we chose two sets of parameters separately. Here, since we aim to provide a systematic description of all the decuplet

baryons, the parameters are re-determined. We simply keep the parameters c_2, c_3, and m_R in Ref. [61] for Ω hyperon (the s quark system) and re-determine the parameters associated to the light-flavor, such as m_u, m_{ud}, and m_{us}, since the mass of Δ is defined as the average between Δ and nucleon instead of its physical mass in Ref. [59].

In this work, all the decuplet baryon masses M are chosen from Ref. [2]. To ensure that the quark and the diquark are in bound states, the input masses of the quark and diquark need to satisfy the relation $M < m_q + m_D$ and $m_D < m_{q_a} + m_{q_b}$. Since m_R is positively correlated with the baryon mass and has little effect on the results [59,61], we simply borrow $m_R = 2.2$ GeV from our previous work about the heaviest baryon Ω^- [61].

As shown in Fig. 3a, c_2, c_3 have little impact on the electric-monopole and magnetic-dipole form factors. When c_2 and c_3 (in units of GeV^{-1} and GeV^{-2}, respectively) run from 0 to 1, the value of $G_{M1}^{\Delta^+}(0)$ changes by only about 3%. However, the higher-order multipoles, especially the magnetic-octupole form factor $G_{M3}(t)$, are sensitive to the values of c_2 and c_3. According to Fig. 3c, $G_{M3}^{\Delta^+}(0)$ even changes its sign as the two parameters increase. Here we keep the same parameters from our previous work about Ω^- [61], $c_2 = 0.306$ GeV^{-1} and $c_3 = 0.056$ GeV^{-2}, which were obtained by fitting to the LQCD data on the electric-monopole, electric-quadrupole, and magnetic-dipole form factors. Since the experimental and empirical LQCD results of $G_{M3}(t)$ are still lacking, our c_2 and c_3 are only roughly determined.

Finally, we have one set of parameters to describe the EMFFs and the GFFs of all the decuplet baryons simultaneously in Table 1, where $m_{q_1q_2}$ stands for the mass of the diquark composed of q_1 and q_2, and we assume that $m_d = m_u$, $m_{us} = m_{ds}$, and $m_{uu} = m_{ud} = m_{dd}$.
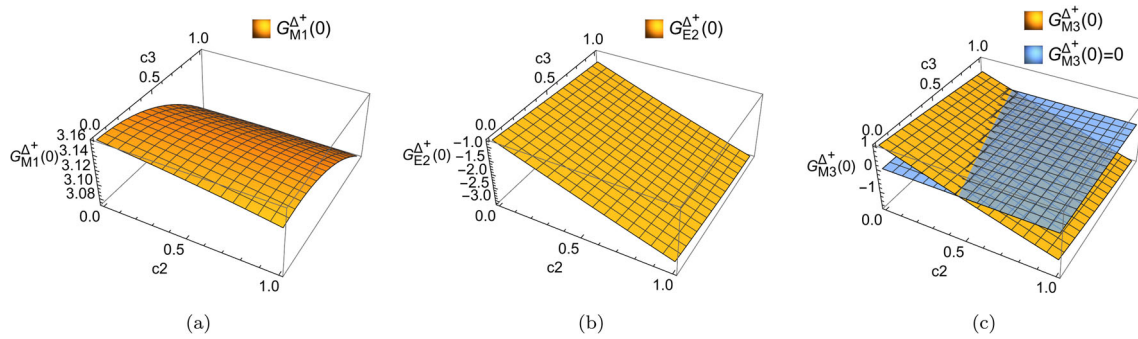
Fig. 3 $G_{M1}^{\Delta^+}(0)$, $G_{E2}^{\Delta^+}(0)$, and $G_{M3}^{\Delta^+}(0)$ as the parameters c_2 and c_3 (in units of GeV^{-1} and GeV^{-2}, respectively) change

Table 1 Parameters used in this work

M_Δ/GeV	M_{Σ^*}/GeV	M_{Ξ^*}/GeV	M_Ω/GeV	m_u/GeV	m_s/GeV
1.232	1.385	1.530	1.672	0.43	0.6
m_{ud}/GeV	m_{us}/GeV	m_{ss}/GeV	m_R/GeV	c_2/GeV^{-1}	c_3/GeV^{-2}
0.82	0.99	1.15	2.2	0.306	0.056

3.2 EMFFs numerical results

Here we show our calculated results of the EMFFs of the decuplet baryons. In Fig. 4, our EMFFs of Δ^+ are qualitatively consistent with the LQCD results of Ref. [36] and also with our previous calculation in Ref. [59].[2] The figures also show the quark and the diquark contributions separately. Since Δ^+ is composed of both $u(ud)$ and $d(uu)$, the value is their average according to the wave function in Appendix A. Figures 5 and 6 plot the EMFFs of other different isospin states of Σ^* and Ξ^*. For isovectors of Σ^{*+}, Σ^{*0} and Σ^{*-}, we employ the same normalization constant $\mathcal{C}$ to ensure $G_{E0}^{\Sigma^{*+}}(0) = 1$. As seen in the first panel in Fig. 5, $G_{E0}(0)$ of Σ^{*0} and Σ^{*-} are very close to 0 and -1, respectively, indicating that the normalization condition is nearly satisfied. Similar results occur for Ξ^*. It should be specifically mentioned that our EMFF results of Δ^0 are strictly zero; however, those of Σ^{*0} and Ξ^{*0} are close to but not exactly zero because of to s and $u(d)$ having different masses, which breaks the SU(3) symmetry slightly. Since the form factors of Ω^- were calculated with the same set of parameters and shown in our previous work [61], we do not address them here for simplicity.

Tables 2 and 3 list the electric charge and magnetic radii obtained from our work and other studies including LQCD [36–38], the chiral quark model [51], and $1/N_c$ expansion [52,53]. Compared with other works, our results are generally larger but qualitatively consistent with theirs. In our previous study on the Δ resonance [14], we chose the baryon

mass as $M = 1.085$ GeV, which is the average of $\Delta(1232)$ and nucleon. Since we choose a different set of parameters for u and d quarks in this work, the charge radius of $\Delta(1232)$ here is slightly larger than that in Ref. [14]. It is seen that, for Δ^-, Σ^{*-}, Ξ^{*-}, and Ω^- hyperons, the electric charge and magnetic radii decrease in turn. This feature may be attributable to the different binding strengths of the baryons. Ω^- has the longest lifetime in the decuplets, suggesting that its binding strengths are the strongest. Consequently, the location of quarks inside Ω^- may be very close to the origin and lead to the smallest radius. Similarly, for the Δ, Σ^*, and Ξ^* isobars, the larger decay width indicates a less stable structure, which leads to the larger radius.

The magnetic moments of all the decuplets, compared with those from other theoretical and experimental works, are presented in Table 4. It can be seen that ours are qualitatively consistent with the experiments and other studies. Table 5 shows the electric quadrupole moments, whose sign characterizes the deformation of the charge distribution. A positive value suggests that the particle has a prolate charge distribution and, contrarily, a negative value stands for an oblate shape. To sum up, we find that all the baryons with a positive charge have negative electric quadrupole moments, and negatively charged baryons are the opposite. Note that the obtained moments are the so-called spectroscopic moments, which are measured in the laboratory. Therefore, the shape discussed in this paper is the spectroscopic shape instead of the geometric shape derived from the intrinsic quadrupole moments [70,71].

---

[2] Our $G_{E0}(t)$ are smaller than the lattice results. It should be mentioned that Ref. [36] gives the Δ isobar mass as about 1.5 GeV, which is about 30% overestimated.
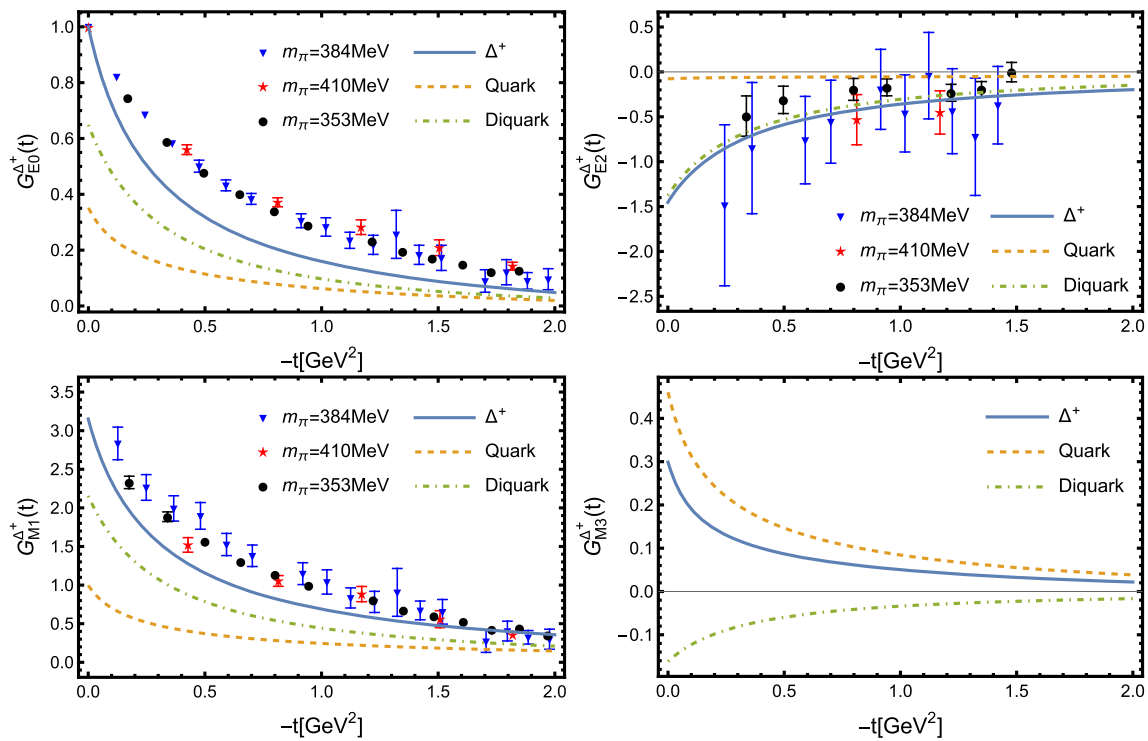
Fig. 4 EMFFs of Δ^+, compared with the LQCD results [36]. The solid, dashed, and dot-dashed curves represent the total EMFFs and those contributed by quark and diquark
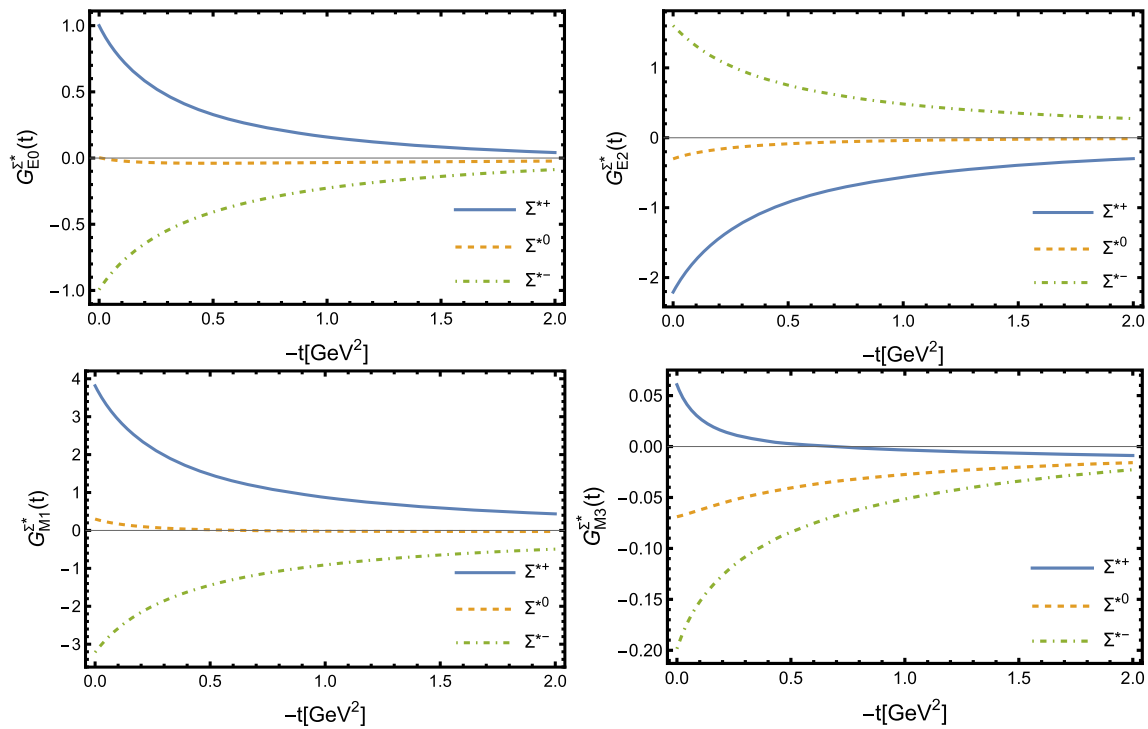

Fig. 5 EMFFs of Σ^*. The solid, dashed and dot-dashed curves represent the EMFFs of Σ^{*+}, Σ^{*0}, and Σ^{*-}

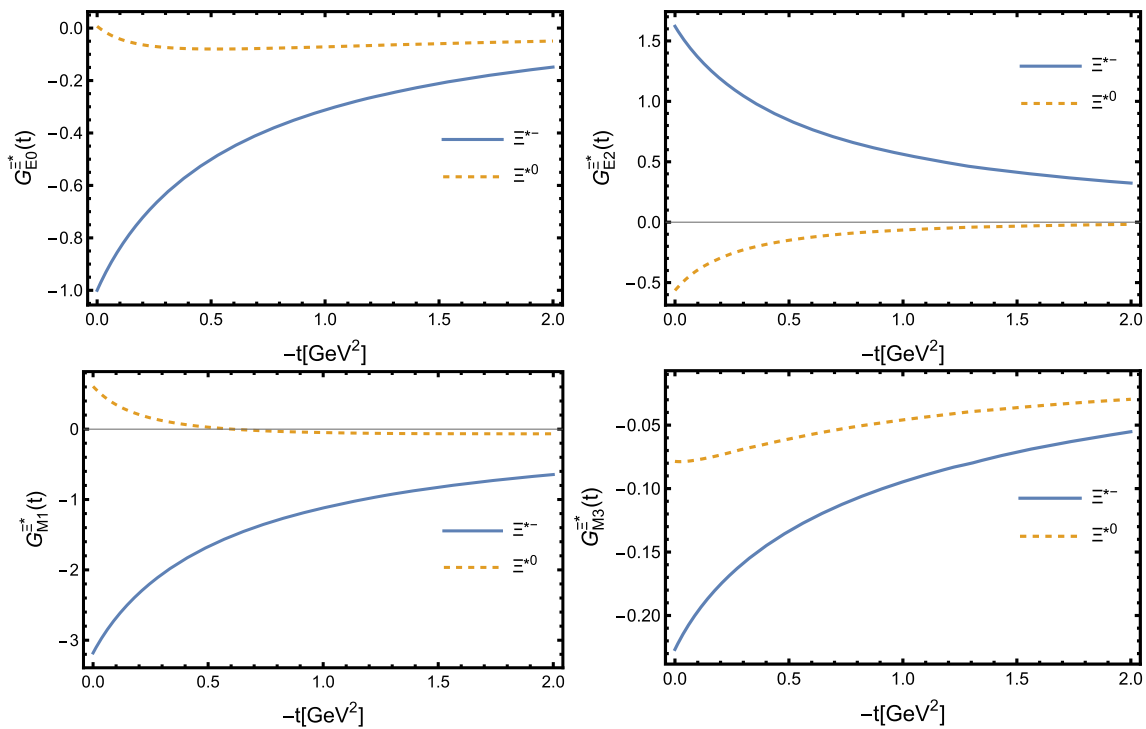**Fig. 6** EMFFs of Ξ^*. The solid and dashed curves represent the EMFFs of Ξ^{*-} and Ξ^{*0}

Table 2 Electric charge radii of the decuplet baryons, compared with those from LQCD [36–38], chiral perturbation theory [43,44], the chiral constituent quark model [46], chiral quark model [51], $1/N_c$ expansion [52,53], and chiral quark-soliton model [56]

$\langle r^2 \rangle_{E0}$/fm^2	Δ^{++}	Δ^+	Δ^0	Δ^-	Σ^{*+}	Σ^{*0}	Σ^{*-}	Ξ^{*0}	Ξ^{*-}	Ω^-
This work	0.894	0.894	0	0.894	0.784	0.087	0.614	0.166	0.451	0.361
LQCD [36,37]	$\cdots$	0.641(22)	$\cdots$	$\cdots$	$\cdots$	$\cdots$	$\cdots$	$\cdots$	$\cdots$	0.355(14)
LQCD [38]	$\cdots$	0.410(57)	0	$\cdots$	0.399(45)	0.020(7)	0.360(32)	0.043(10)	0.330(20)	0.307(15)
χPT [43]	0.325(22)	0.328(21)	0.006(1)	0.316(23)	0.315(21)	0	0.315(21)	$-0.006(1)$	0.312(18)	0.307(15)
χPT [44]	0.30(11)	0.29(10)	$-0.02(1)$	0.33(11)	0.31(11)	0	0.31(11)	0.02(1)	0.29(10)	0.27(10)
χCQM [46]	0.43	0.43	0	0.43	0.42	0.37	0.03	0.06	0.33	0.29
χQM [51]	0.77	0.77	0	0.77	0.93	0.10	0.74	0.20	0.68	0.78
$1/N_c$ [52]	1.048	1.101	0.105	0.891	0.939	-0.031	0.895	-0.098	0.981	1.042
$1/N_c$ [53]	0.783	0.783	0	0.783	0.869	0.108	0.669	0.206	0.561	0.457
χQSM [56]	0.826	0.792	-0.069	0.930	0.843	-0.024	0.891	0.021	0.852	0.813

Table 3 Magnetic radii of the decuplet baryons, compared with those from LQCD [37], chiral perturbation theory [44], the chiral quark model [51], and chiral quark-soliton model [56]

$\langle r^2 \rangle_{M1}$/fm^2	Δ^{++}	Δ^+	Δ^0	Δ^-	Σ^{*+}	Σ^{*0}	Σ^{*-}	Ξ^{*0}	Ξ^{*-}	Ω^-
This work	0.827	0.827	0	0.827	0.703	0.421	0.573	0.820	0.443	0.340
LQCD [37]	$\cdots$	$\cdots$	$\cdots$	$\cdots$	$\cdots$	$\cdots$	$\cdots$	$\cdots$	$\cdots$	0.286(31)
χPT [44]	0.61(15)	0.64(14)	0.07(12)	0.55(19)	0.59(16)	0	0.59(16)	$-0.07(12)$	0.64(14)	0.70(12)
χQM [51]	0.62	0.62	0	0.62	0.67	0.82	0.61	0.82	0.58	0.53
χQSM [56]	0.587	0.513	1.786	0.764	0.599	3.356	0.713	0.784	0.653	0.582

Table 4 Magnetic moments of the decuplet baryons, compared with those from PDG [2], LQCD [36–41], chiral perturbation theory [43,44], the relativistic quark model [47], QCD sum rules [49], chiral quark model [51], chiral quark-soliton model [56], and $1/N_c$ expansion [73]

μ/μ_N	Δ^{++}	Δ^+	Δ^0	Δ^-	Σ^{*+}	Σ^{*0}	Σ^{*-}	Ξ^{*0}	Ξ^{*-}	Ω^-
This work	4.80	2.40	0	−2.40	2.58	0.20	−2.18	0.37	−1.95	−1.79
PDG [2]	6.14(51)	$2.7^{+1.0}_{-1.3} \pm 1.5 \pm 3$	$\cdots$	$\cdots$	$\cdots$	$\cdots$	$\cdots$	$\cdots$	$\cdots$	−2.02(5)
LQCD [36,37]	$\cdots$	1.91(16)	$\cdots$	$\cdots$	$\cdots$	$\cdots$	$\cdots$	$\cdots$	$\cdots$	−1.835(94)
LQCD [38]	3.20(56)	1.60(28)	0	−1.60(28)	1.76(18)	0.00(4)	−1.75(13)	0.08(5)	−1.76(8)	−1.70(7)
LQCD [39]	3.70(12)	2.40(6)	$\cdots$	−1.85(6)	$\cdots$	$\cdots$	$\cdots$	$\cdots$	$\cdots$	−1.93(8)
LQCD [40]	4.91(61)	2.46(31)	0.00	−2.46(31)	2.55(26)	0.27(5)	−2.02(18)	0.46(7)	−1.68(12)	−1.40(10)
LQCD [41]	5.24(18)	0.97(8)	−0.035(2)	−2.98(19)	1.27(6)	0.33(5)	−1.88(4)	0.16(4)	−0.62(1)	$\cdots$
χPT [43]	6.04(13)	2.84(2)	−0.36(9)	−3.56(20)	3.07(12)	0	−3.07(12)	0.36(9)	−2.56(6)	−2.02
χPT [44]	4.97(89)	2.60(50)	0.02(12)	−2.48(32)	1.76(38)	−0.02(3)	−1.85(38)	−0.42(13)	−1.90(47)	−2.02(5)
RQM [47]	4.76	2.38	0	−2.38	1.82	−0.27	−2.36	−0.60	−2.41	−2.35
QCDSR [49]	4.13(1.30)	2.07(65)	0	−2.07(65)	2.13(82)	−0.32(15)	−1.66(73)	−0.69(29)	−1.51(52)	−1.49(45)
χQM [51]	6.93	3.47	0	−3.47	4.12	0.53	−3.06	1.10	−2.61	−2.13
χQSM [56]	3.65	1.72	−0.21	−2.14	1.91	−0.04	−1.99	0.13	−1.84	−1.69
HBχPT [72]	4.0(4)	2.1(2)	−0.17(4)	−2.25(25)	2.0(2)	−0.07(2)	−2.2(2)	0.10(4)	−2.0(2)	−1.94(22)
$1/N_c$ [73]	5.9(4)	2.9(2)	$\cdots$	−2.9(2)	3.3(2)	0.3(1)	−2.8(3)	0.65(20)	−2.30(15)	−1.94

Table 5 Electric-quadrupole moments of the decuplet baryons compared with those from LQCD [36,37], the Skyrme model [42], nonrelativistic quark model [45], QCD sum rules [48,50], chiral quark model [51], $1/N_c$ expansion [53], general QCD parameterization method [54], chiral quark-soliton model [56], and chiral perturbation theory [72]

$\mathcal{Q}/\text{fm}^2$	Δ^{++}	Δ^+	Δ^0	Δ^-	Σ^{*+}	Σ^{*0}	Σ^{*-}	Ξ^{*0}	Ξ^{*-}	Ω^-
This work	−0.075	−0.037	0	0.037	−0.045	−0.006	0.033	−0.009	0.027	0.024
LQCD [36,37]	$\cdots$	−0.019(17)	$\cdots$	$\cdots$	$\cdots$	$\cdots$	$\cdots$	$\cdots$	$\cdots$	0.019(3)
Skyrme [42]	−0.088	−0.029	0.029	0.088	−0.071	0	0.071	−0.046	0.046	0
NQM [45]	−0.093	−0.046	0	0.046	−0.054	−0.007	0.040	−0.013	0.034	0.028
QCDSR [48,50]	−0.028(8)	−0.014(4)	0	0.014(4)	−0.028(9)	0.0012(4)	0.03(1)	0.0025(8)	0.045(15)	0.12(4)
χQM [51]	−0.252	−0.126	0	0.126	−0.123	−0.021	0.082	−0.030	0.048	0.026
$1/N_c$ [53]	−0.120	−0.060	0	0.060	−0.069	0.014	0.077	−0.023	0.047	0.027
GPM [54]	−0.226	−0.113	0	0.113	−0.107	−0.017	0.074	−0.023	0.044	0.024
χQSM [56]	−0.102	−0.039	0.023	0.085	−0.070	0.003	0.077	−0.016	0.069	0.061
HBχPT [72]	−0.08(5)	−0.03(2)	0.012(5)	0.06(3)	−0.07(3)	−0.013(7)	0.04(2)	−0.035(2)	0.02(1)	0.009(5)

3.3 GMFF numerical results

Figure 7 shows the obtained GMFFs including energy-monopole $\varepsilon_0(t)$, energy-quadrupole $\varepsilon_2(t)$, angular momentum-dipole $\mathcal{J}_1(t)$, and the D-term correlated $D_0(t)$. We employ the same normalization constant $\mathcal{C}$ and $\mathcal{C}_D$ as with those in EMFFs determined in Sect. 3.2. It is seen that for all the decuplet baryons, $\varepsilon_0(0)$ and $\mathcal{J}(0)$ run from 0.97 to 0.99 and from 1.46 to 1.48 separately, which are almost consistent with the normalization condition $\varepsilon_0(0) = 1$ and $\mathcal{J}(0) = 3/2$. As discussed in Refs. [24,74], the momentum-dependent scalar function introduced in Eq. (15) may break the gauge invariance and the electromagnetic Ward–Takahashi identity, and consequently the EMFFs and GFFs cannot be normalized at the same time. Similar to the discussion of the electric-

quadrupole moment, the positive energy-quadrupole moment $\varepsilon_2(0)$ suggests that all the decuplet baryons have a prolate mass distribution.

Figure 8 shows the energy-monopole and angular momentum-dipole form factors of Σ^{*+} with the quark and the diquark contributions plotted, respectively. According to Fig. 8, the angular-momentum contribution of the diquark is about twice that of the quark, especially when t goes to 0. This phenomenon is consistent with our understanding of baryon spin, since the decuplet baryons are composed of a spin-1/2 quark and a spin-1 diquark.

According to the definition in Eq. (6), we can further derive the mass radii of the baryons as shown in Table 6. Compared with the electric charge and magnetic radii in Tables 2 and 3,
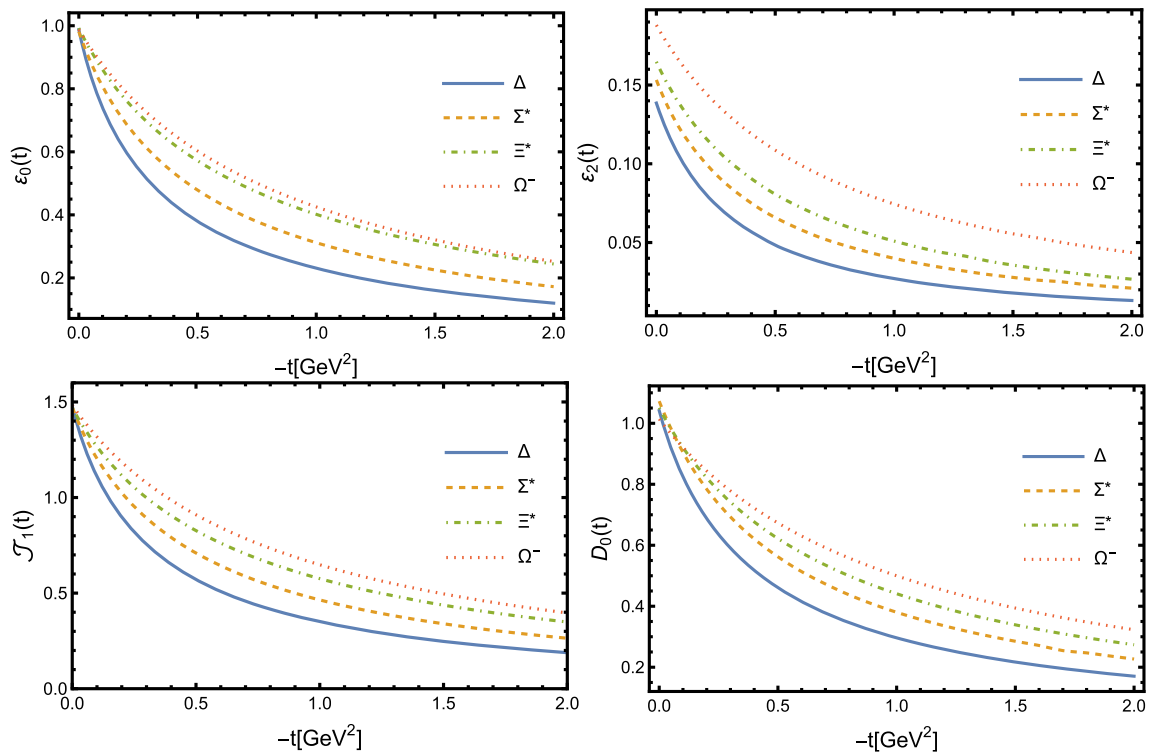
Fig. 7 GMFFs of the decuplet baryons. The solid, dashed, dot-dashed, and dotted curves represent the GMFFs of Δ, Σ^*, Ξ^*, and Ω^-
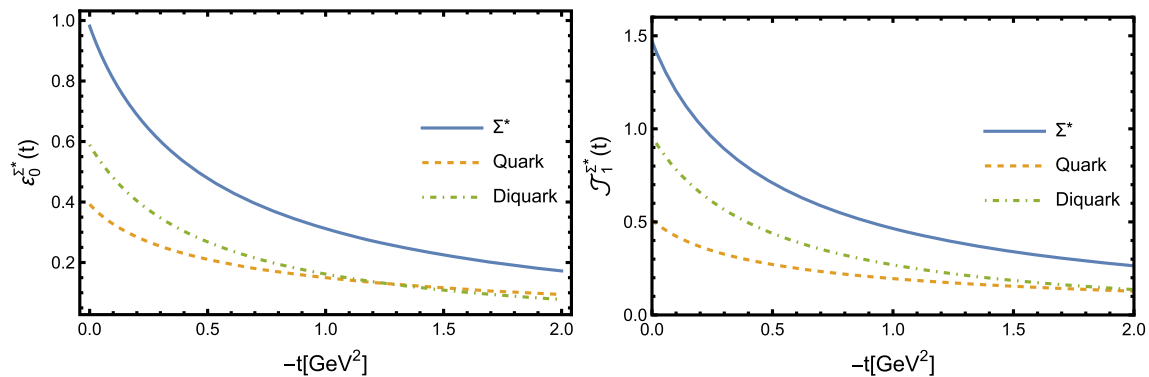

Fig. 8 The energy-monopole and angular momentum form factors of Σ^*. The solid, dashed, and dot-dashed curves represent the total GMFFs and those contributed by quark and diquark

the mass radii are slightly smaller. Similarly, the mass radius becomes smaller as the mass increases.

The energy density, angular momentum density, and strong force density in the r-space inside the baryon can also be derived through the Fourier transformation. References [75–77] suggest that the local density distribution must depend on the size of the wave packet of the system. An additional wave packet is necessary, physically and mathematically, to guarantee the convergence of the Fourier transformation. Of course, the wave package introduces a new parameter λ and may have an influence on the definition of the radius [75,78]. However, this issue is not a priority in this work.

Here we simply follow the idea of Refs. [75–77] and employ a Gaussian-like wave packet e^{t/λ^2} [79]. The parameter λ has the mass dimension, and $1/\lambda$ correlates with the size of the hadron. As seen in Table 6, the mass radii of the baryons become smaller as their masses increase. Reference [76] has a detailed discussion on the determination of λ. For convenience and simplicity, we assume that $1/\lambda$ roughly relates to the Compton length of the system. and there is a linear relation between the mass radius and $1/\lambda$ of the baryon

$$\sqrt{\langle r^2 \rangle_M} = \alpha \frac{1}{\lambda}, \tag{25}$$

Table 6 Mass radii of the decuplet baryons

$\langle r^2 \rangle_M / \text{fm}^2$	Δ	Σ^*	Ξ^*	Ω^-
This work	0.801	0.516	0.368	0.298

where the parameter $\alpha \sim 4$ is employed in our numerical calculation.

Figure 9 shows the energy-monopole densities and angular momentum densities of the decuplet baryons. The integrated result of $\mathcal{E}_0(r)$ and $\rho_J(r)$ over the whole coordinate space gives the mass and spin of the corresponding baryon. The right panel gives the angular momentum densities of the baryons, where it is seen that the large λ concentrates the densities close to the origin.

Finally, $D_{0,2,3}(t)$ are supposed to connect with the pressure and shear force in the classical physical concept discussed in Ref. [1]. As shown in Fig. 7, the D-term, $D = D_0(0)$, of all the baryons is positive. However, it is argued in Ref. [58] that the D-term should be negative in order to guarantee the stability of the system. The sign of the present D-term is consistent with our previous results [59,61] in the same quark–diquark approach, and with the result of the hydrogen atom [80]. Although the phenomenon of $D > 0$ is not consistent with the arguments in Ref. [58], it still satisfies the von Laue condition $\int_0^\infty \mathrm{d}r\, r^2 p_0(r) = 0$. Here, we argue that the classical definitions of the pressure and shear force may not exist in the few-body system we are dealing with, because they are derived from statistical means in classical multi-body systems. The hydrogen atom is also a few-body system, so its non-positive D-term is not necessary. A more detailed discussion is given in our work on Ω^- in Ref. [61].

4 Summary and discussion

In this work, the EMFFs and GFFs of all the decuplet baryons have been calculated systematically and simultaneously with a relativistic covariant quark–diquark approach. The baryon structure is simplified from a three-body system into a two-body system, which effectively simplifies our calculations. To ensure the bound state between the quark and the diquark, an additional scalar function is used. Although this scalar function may have an impact on the gauge invariance, the deviation of the normalization in our numerical results is small.

We then fit our results of the EMFFs to the LQCD calculations for Δ^+ and Ω^- and try to find a set of parameters that give a systematic and reasonable description of all the decuplet baryons. Here, we simply keep the parameters for the s quark system of Ω^- and recalculate the others containing u and d quarks. The model parameters cannot be rigorously determined due to the lack of experimental and LQCD data on the strongly parameter-dependent higher-order multipole form factors.

In the numerical calculations, we obtain the electromagnetic properties including electric charge radii, magnetic moments, electric-quadrupole moments, and magnetic octupole moments, which are in reasonable agreement with those from some experiments, LQCD calculations, and other models. We also calculate the GMFFs of the decuplet baryons, and derive the mechanical properties of the systems, including their mass radii, energy, and angular momentum distributions. This shows that the mass radius is smaller than the electromagnetic radius for all the baryons, and the mass radii decrease as the baryon masses increase. More-
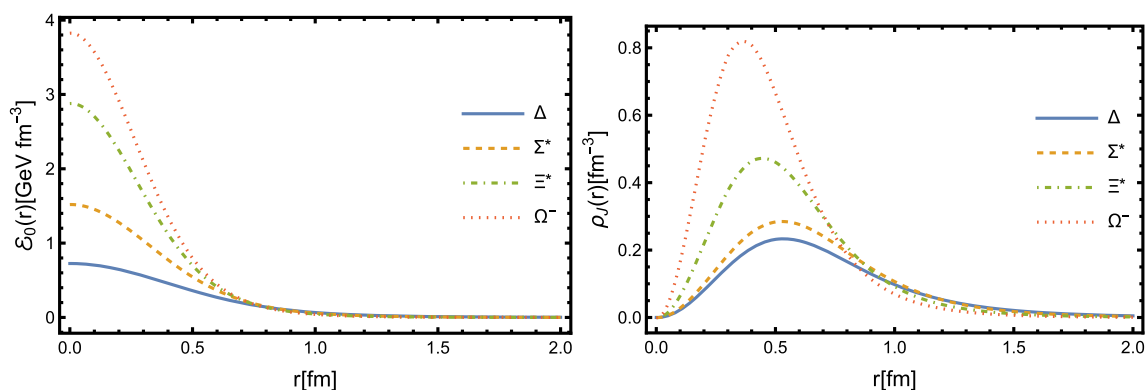

Fig. 9 The energy-monopole and angular momentum densities of the decuplet baryons. The solid, dashed, dot-dashed, and dotted curves represent the densities of Δ, Σ^*, Ξ^*, and Ω^-

over, the distributions in the coordinate space for the energy and angular momentum distributions are also shown with the introduction of an effective wave package. The sign of the D-terms in our approach remains positive, though how to understand this is still controversial.

It is expected that the present systematic description of the EMFFs and GFFs for all the decuplet baryons might provide more useful information to comprehend the inner structure of those baryons with spin-3/2, and also provide reference for future possible experiments at EIC, EicC, and JPARC.

Data Availability Statement This manuscript has no associated data or the data will not be deposited. [Authors' comment: Since the results in this work are obtained theoretically, this manuscript has no associated data.]

Appendix A: SU(6) wave functions of the decuplets

In the quark–diquark approach, the spin-isospin SU(6) wave functions of the decuplets are expressed as [65]

$$|\Delta^{++}\rangle = |u(uu)\rangle\,\phi, \tag{A1}$$

$$|\Delta^{+}\rangle = \left(\sqrt{\frac{2}{3}}\,|u(ud)\rangle + \sqrt{\frac{1}{3}}\,|d(uu)\rangle\right)\phi, \tag{A2}$$

$$|\Delta^{0}\rangle = \left(\sqrt{\frac{2}{3}}\,|d(ud)\rangle + \sqrt{\frac{1}{3}}\,|u(dd)\rangle\right)\phi, \tag{A3}$$

$$|\Delta^{-}\rangle = |d(dd)\rangle\,\phi, \tag{A4}$$

$$|\Sigma^{*+}\rangle = \left(\sqrt{\frac{2}{3}}\,|u(us)\rangle + \sqrt{\frac{1}{3}}\,|s(uu)\rangle\right)\phi, \tag{A5}$$

$$|\Sigma^{*0}\rangle = \left(\sqrt{\frac{1}{3}}\,|d(us)\rangle + \sqrt{\frac{1}{3}}\,|u(ds)\rangle + \sqrt{\frac{1}{3}}\,|s(ud)\rangle\right)\phi, \tag{A6}$$

$$|\Sigma^{*-}\rangle = \left(\sqrt{\frac{2}{3}}\,|d(ds)\rangle + \sqrt{\frac{1}{3}}\,|s(dd)\rangle\right)\phi, \tag{A7}$$

$$|\Xi^{*0}\rangle = \left(\sqrt{\frac{2}{3}}\,|s(us)\rangle + \sqrt{\frac{1}{3}}\,|u(ss)\rangle\right)\phi, \tag{A8}$$

$$|\Xi^{*-}\rangle = \left(\sqrt{\frac{2}{3}}\,|s(ds)\rangle + \sqrt{\frac{1}{3}}\,|d(ss)\rangle\right)\phi, \tag{A9}$$

$$|\Omega^{-}\rangle = |s(ss)\rangle\,\phi, \tag{A10}$$

where ϕ is the spin wave function and $(q_a q_b)$ stands for the axial-vector diquark which is composed of quarks q_a and q_b.

References

1. M.V. Polyakov, P. Schweitzer, Forces inside hadrons: pressure, surface tension, mechanical radius, and all that. Int. J. Mod. Phys. A **33**(26), 1830025 (2018)
2. R.L. Workman et al., Review of particle physics. PTEP **2022**, 083C01 (2022)
3. G. Blanpied et al., N → Delta transition from simultaneous measurements of p (gamma →, pi) and p (gamma →, gamma). Phys. Rev. Lett. **79**, 4337–4340 (1997)
4. K. Joo et al., Q**2 dependence of quadrupole strength in the gamma* p → Delta+(1232) → p pi0 transition. Phys. Rev. Lett. **88**, 122001 (2002)
5. N. Sparveris et al., Measurements of the γ*p → Δ reaction at low Q^2. Eur. Phys. J. A **49**, 136 (2013)
6. G. Lopez Castro, A. Mariano, Determination of the Delta++ magnetic dipole moment. Phys. Lett. B **517**, 339–344 (2001)
7. M. Kotulla et al., The Reaction gamma p → pi zero gamma-prime p and the magnetic dipole moment of the delta+(1232) resonance. Phys. Rev. Lett. **89**, 272001 (2002)
8. S. Dobbs, A. Tomaradze, T. Xiao, Kamal K. Seth, G. Bonvicini, First measurements of timelike form factors of the hyperons, Λ^0, Σ^0, Σ^+, Ξ^0, Ξ^-, and Ω^-, and evidence of diquark correlations. Phys. Lett. B **739**, 90–94 (2014)
9. BESIII Collaboration, Study of $e^+e^- \to \Omega^-\overline{\Omega}^+$ at center-of-mass energies from 3.49 to 3.67 GeV. Phys. Rev. D **107**, 052003 (2023)
10. C.-Z. Yuan, M. Karliner, Cornucopia of antineutrons and hyperons from a super j/ψ factory for next-generation nuclear and particle physics high-precision experiments. Phys. Rev. Lett. **127**, 012003 (2021)
11. L. Guo et al., Cascade production in the reactions $\gamma p \to K^+K^+(x)$ and $\gamma p \to K^+K^+\pi^-(x)$. Phys. Rev. C **76**, 025208 (2007)
12. J.T. Goetz et al., Study of Ξ^* photoproduction from threshold to $W = 3.3$ GeV. Phys. Rev. C **98**(6), 062201 (2018)
13. M. Diehl, Generalized parton distributions. Phys. Rep. **388**, 41–277 (2003)
14. D. Fu, B.-D. Sun, Y. Dong, Generalized parton distributions in spin-3/2 particles. Phys. Rev. D **106**(11), 116012 (2022)
15. B.-D. Sun, Y.-B. Dong, Gravitational form factors of ρ meson with a light-cone constituent quark model. Phys. Rev. D **101**, 096008 (2020)

16. D. Fu, B.-D. Sun, Y. Dong, Generalized parton distributions of Δ resonance in a diquark spectator approach. Phys. Rev. D **107**(11), 116021 (2023)

17. S. Kumano, Q.-T. Song, O.V. Teryaev, Hadron tomography by generalized distribution amplitudes in the pion-pair production process $\gamma^*\gamma \to \pi^0\pi^0$ and gravitational form factors for pion. Phys. Rev. D **97**, 014020 (2018)

18. X.-D. Ji, Off forward parton distributions. J. Phys. G **24**, 1181–1205 (1998)

19. V.D. Burkert, L. Elouadrhiri, F.X. Girod, The pressure distribution inside the proton. Nature **557**(7705), 396–399 (2018)

20. A. Prokudin, Y. Hatta, Y. Kovchegov, C. Marquet, *Probing Nucleons and Nuclei in High Energy Collisions* (World Scientific, Singapore, 2020)

21. X. Chen, A plan for electron ion collider in China. PoS **DIS2018**, 170 (2018)

22. G. Hohler, E. Pietarinen, Electromagnetic radii of nucleon and pion. Phys. Lett. B **53**, 471–475 (1975)

23. P. Maris, P.C. Tandy, The pi, K+, and K0 electromagnetic form-factors. Phys. Rev. C **62**, 055204 (2000)

24. W. Broniowski, E.R. Arriola, Gravitational and higher-order form factors of the pion in chiral quark models. Phys. Rev. D **78**, 094011 (2008)

25. A.M. Bincer, Electromagnetic structure of the nucleon. Phys. Rev. **118**, 855–863 (1960)

26. V. Keiner, A covariant diquark–quark model of the nucleon in the Salpeter approach. Phys. Rev. C **54**, 3232–3239 (1996)

27. H. Meyer, The nucleon as a relativistic quark–diquark bound state with an exchange potential. Phys. Lett. B **337**, 37–42 (1994)

28. B.-Q. Ma, D. Qing, I. Schmidt, Electromagnetic form factors of nucleons in a light-cone diquark model. Phys. Rev. C **65**(3), 035205 (2002)

29. H.-C. Kim, P. Schweitzer, U. Yakhshiev, Energy-momentum tensor form factors of the nucleon in nuclear matter. Phys. Lett. B **718**(2), 625–631 (2012)

30. K. Goeke, J. Grabis, J. Ossmann, M.V. Polyakov, P. Schweitzer, A. Silva, D. Urbano, Nucleon form-factors of the energy momentum tensor in the chiral quark-soliton model. Phys. Rev. D **75**(9), 094021 (2007)

31. L.E. Marcucci, F. Gross, M.T. Pena, M. Piarulli, R. Schiavilla, I. Sick, A. Stadler, J.W. Van Orden, M. Viviani, Electromagnetic structure of few-nucleon ground states. J. Phys. G **43**, 023002 (2016)

32. W. Cosyn, A. Freese, B. Pire, Polynomiality sum rules for generalized parton distributions of spin-1 targets. Phys. Rev. D **99**, 094035 (2019)

33. B.-D. Sun, Y.-B. Dong, ρ meson unpolarized generalized parton distributions with a light-front constituent quark model. Phys. Rev. D **96**(3), 036019 (2017)

34. Y. Dong, C. Liang, Generalized parton distribution functions of a deuteron in a phenomenological Lagrangian approach. J. Phys. G **40**, 025001 (2013)

35. M.V. Polyakov, B.-D. Sun, Gravitational form factors of a spin one particle. Phys. Rev. D **100**, 036003 (2019)

36. C. Alexandrou, T. Korzec, G. Koutsou, Th. Leontiou, C. Lorcé, J.W. Negele, V. Pascalutsa, A. Tsapalis, M. Vanderhaeghen, Δ-baryon electromagnetic form factors in lattice QCD. Phys. Rev. D **79**, 014507 (2009)

37. C. Alexandrou, T. Korzec, G. Koutsou, J.W. Negele, Y. Proestos, The electromagnetic form factors of the Ω^- in lattice QCD. Phys. Rev. D **82**, 034504 (2010)

38. S. Boinepalli, D.B. Leinweber, P.J. Moran, A.G. Williams, J.M. Zanotti, J.B. Zhang, Precision electromagnetic structure of decuplet baryons in the chiral regime. Phys. Rev. D **80**, 054505 (2009)

39. C. Aubin, K. Orginos, V. Pascalutsa, M. Vanderhaeghen, Lattice calculation of the magnetic moments of Δ and Ω^- baryons with dynamical clover fermions. Phys. Rev. D **79**, 051502 (2009)

40. D.B. Leinweber, T. Draper, R.M. Woloshyn, Decuplet baryon structure from lattice QCD. Phys. Rev. D **46**, 3067–3085 (1992)

41. F.X. Lee, R. Kelly, L. Zhou, W. Wilcox, Baryon magnetic moments in the background field method. Phys. Lett. B **627**, 71–76 (2005)

42. Y. Oh, Electric quadrupole moments of the decuplet baryons in the Skyrme model. Mod. Phys. Lett. A **10**, 1027–1034 (1995)

43. L.S. Geng, J. Martin Camalich, M.J. Vicente Vacas, Electromagnetic structure of the lowest-lying decuplet resonances in covariant chiral perturbation theory. Phys. Rev. D **80**, 034027 (2009)

44. H.-S. Li, Z.-W. Liu, X.-L. Chen, W.-Z. Deng, S.-L. Zhu, Magnetic moments and electromagnetic form factors of the decuplet baryons in chiral perturbation theory. Phys. Rev. D **95**(7), 076001 (2017)

45. M.I. Krivoruchenko, M.M. Giannini, Quadrupole moments of the decuplet baryons. Phys. Rev. D **43**, 3763–3765 (1991)

46. K. Berger, R.F. Wagenbrunn, W. Plessas, Covariant baryon charge radii and magnetic moments in a chiral constituent quark model. Phys. Rev. D **70**, 094027 (2004)

47. F. Schlumpf, Magnetic moments of the baryon decuplet in a relativistic quark model. Phys. Rev. D **48**, 4478–4480 (1993)

48. T.M. Aliev, K. Azizi, M. Savci, Electric quadrupole and magnetic octupole moments of the light decuplet baryons within light cone QCD sum rules. Phys. Lett. B **681**, 240–246 (2009)

49. F.X. Lee, Determination of decuplet baryon magnetic moments from QCD sum rules. Phys. Rev. D **57**, 1801–1821 (1998)

50. K. Azizi, Magnetic dipole, electric quadrupole and magnetic octupole moments of the Delta baryons in light cone QCD sum rules. Eur. Phys. J. C **61**, 311–319 (2009)

51. G. Wagner, A.J. Buchmann, A. Faessler, Electromagnetic properties of decuplet hyperons in a chiral quark model with exchange currents. J. Phys. G **26**, 267–293 (2000)

52. R. Flores-Mendieta, M.A. Rivera-Ruiz, Dirac form factors and electric charge radii of baryons in the combined chiral and $1/N_c$ expansions. Phys. Rev. D **92**(9), 094026 (2015)

53. A.J. Buchmann, R.F. Lebed, Baryon charge radii and quadrupole moments in the 1/N(c) expansion: the three flavor case. Phys. Rev. D **67**, 016002 (2003)

54. A.J. Buchmann, E.M. Henley, Quadrupole moments of baryons. Phys. Rev. D **65**, 073017 (2002)

55. A.J. Buchmann, E.M. Henley, Baryon octupole moments. Eur. Phys. J. A **35**, 267–269 (2008)

56. J.-Y. Kim, H.-C. Kim, Electromagnetic form factors of the baryon decuplet with flavor su(3) symmetry breaking. Eur. Phys. J. C **79**(7), 570 (2019)

57. J.-Y. Kim, B.-D. Sun, Gravitational form factors of a baryon with spin-3/2. Eur. Phys. J. C **81**(1), 85 (2021)

58. I.A. Perevalova, M.V. Polyakov, P. Schweitzer, LHCb pentaquarks as a baryon-$\psi(2s)$ bound state: prediction of isospin-$\frac{3}{2}$ pentaquarks with hidden charm. Phys. Rev. D **94**, 054024 (2016)

59. D. Fu, B.-D. Sun, Y. Dong, Electromagnetic and gravitational form factors of Δ resonance in a covariant quark–diquark approach. Phys. Rev. D **105**, 096002 (2022)

60. Z. Dehghan, K. Azizi, U. Özdem, Gravitational form factors of the Δ baryon via QCD sum rules. Phys. Rev. D **108**(9), 094037 (2023)

61. D. Fu, J.Q. Wang, Y. Dong, Form factors of Ω^- in a covariant quark–diquark approach. Phys. Rev. D **108**, 076023 (2023)

62. S. Cotogno, C. Lorcé, P. Lowdon, M. Morales, Covariant multipole expansion of local currents for massive states of any spin. Phys. Rev. D **101**(5), 056016 (2020)

63. S. Nozawa, D.B. Leinweber, Electromagnetic form-factors of spin 3/2 baryons. Phys. Rev. D **42**, 3567–3571 (1990)

64. G. Ramalho, M.T. Peña, F. Gross, Electric quadrupole and magnetic octupole moments of the δ. Phys. Lett. B **678**(4), 355–358 (2009)

65. D.B. Lichtenberg, L.J. Tassie, P.J. Keleman, Quark–diquark model of baryons and SU(6). Phys. Rev. **167**(5), 1535–1542 (1968)

66. Y. Dong, A. Faessler, T. Gutsche, S. Kovalenko, V.E. Lyubovitskij, $x(3872)$ as a hadronic molecule and its decays to charmonium states and pions. Phys. Rev. D **79**, 094013 (2009)

67. M.D. Scadron, Covariant propagators and vertex functions for any spin. Phys. Rev. **165**(5), 1640–1647 (1968)

68. T. Frederico, E. Pace, B. Pasquini, G. Salmè, Pion generalized parton distributions with covariant and light-front constituent quark models. Phys. Rev. D **80**, 054021 (2009)

69. H. Meyer, The nucleon as a relativistic quark–diquark bound state with an exchange potential. Phys. Lett. B **337**(1–2), 37–42 (1994)

70. A.J. Buchmann, E.M. Henley, Intrinsic quadrupole moment of the nucleon. Phys. Rev. C **63**, 015202 (2001)

71. K. Kumar, Intrinsic quadrupole moments and shapes of nuclear ground states and excited states. Phys. Rev. Lett. **28**, 249–253 (1972)

72. M.N. Butler, M.J. Savage, R.P. Springer, Electromagnetic moments of the baryon decuplet. Phys. Rev. D **49**, 3459–3465 (1994)

73. M.A. Luty, J. March-Russell, M.J. White, Baryon magnetic moments in a simultaneous expansion in 1/N and m(s). Phys. Rev. D **51**, 2332–2337 (1995)

74. R.M. Davidson, E.R. Arriola, Structure functions of pseudoscalar mesons in the SU(3) NJL model. Phys. Lett. B **348**(1), 163–169 (1995)

75. E. Epelbaum, J. Gegelia, N. Lange, U.G. Meißner, M.V. Polyakov, Definition of local spatial densities in hadrons. Phys. Rev. Lett. **129**(1), 012001 (2022)

76. M. Diehl, Generalized parton distributions in impact parameter space. Eur. Phys. J. C **25**(2), 223–232 (2002)

77. A. Freese, G.A. Miller, Unified formalism for electromagnetic and gravitational probes: densities. Phys. Rev. D **105**(1), 014003 (2022)

78. H. Alharazin, B.D. Sun, E. Epelbaum, J. Gegelia, U.G. Meißner, Local spatial densities for composite spin-3/2 systems. JHEP **02**, 163 (2023)

79. T. Ishikawa, L.C. Jin, H.-W. Lin, A. Schäfer, Y.-B. Yang, J.-H. Zhang, Y. Zhao, Gaussian-weighted parton quasi-distribution (Lattice Parton Physics Project (LP^3)). Sci. China Phys. Mech. Astron. **62**(9), 991021 (2019)

80. X. Ji, Y. Liu, Momentum-current gravitational multipoles of hadrons. Phys. Rev. D **106**(3), 034028 (2022)